

Modified empirical fitting of the discharge behavior of LiFePO_4 batteries under various conditions

Shin-Yi Lee¹
Kung-Yen Lee⁴

Wei-Li Chiu²
Jau-Horng Chen⁵
Kang Li⁷

Yi-Shuo Liao³
Huei-Jeng Lin⁶

(Received 31 March 2014; revised 19 June 2014)

Abstract

A mathematical model is developed by fitting the discharge curve of a new LiFePO_4 battery and then used to investigate the relationship between the discharge time and the closed-circuit voltage. This model consists of exponential and polynomial terms where the exponential term dominates the discharge time of a battery and the polynomial term dominates the change in the closed-circuit voltage. Time shift and time scale processes modify the exponential and polynomial terms,

<http://journal.austms.org.au/ojs/index.php/ANZIAMJ/article/view/8182> gives this article, © Austral. Mathematical Soc. 2014. Published August 10, 2014, as part of the Proceedings of the 11th Biennial Engineering Mathematics and Applications Conference. ISSN 1446-8735. (Print two pages per sheet of paper.) Copies of this article must not be made otherwise available on the internet; instead link directly to this URL for this article.

respectively, so that the model is suitable for batteries under various conditions.

Contents

1 Introduction	C369
2 Electrical circuit and mathematical models	C370
3 Results and discussion	C374
4 Conclusions	C380
References	C381

1 Introduction

LiFePO₄ batteries are widely used as energy sources for a variety of devices, including electronic products, electric vehicles and smart grids [1, 2]. A number of battery models intended to capture the characteristics of batteries have been developed, such as the electrochemical model [3, 4], the analytical model [3, 5, 6, 7, 8], the stochastic model [9, 10], and the electrical circuit model [5, 6, 11, 12, 13]. In this article, the electrical circuit model is used to describe the discharge behaviors of LiFePO₄ batteries as it is readily simulated and implemented [12, 13, 14].

A mathematical model based on the electrical circuit model is developed by fitting the closed-circuit voltage (CCV) versus the discharge time curve of a new battery. The developed model consists of exponential and polynomial terms. The model is not suitable for different types of used and aged batteries, so the parameters in the model need to be modified to cater for batteries under various conditions. To transform the model so that it is suitable

for all batteries independent of the conditions, without rederiving these parameters, time shift and time scale processes are applied to the exponential and polynomial terms, respectively. It is much easier to distinguish batteries under various conditions using the time shift and time scale values, compared to rederiving all parameters of the model for each battery condition. The fitting results compared with the experimental data are illustrated.

2 Electrical circuit and mathematical models

An electrical circuit composed of a nonlinear open-circuit voltage source, a series resistor and one resistor-capacitor (RC) network, shown in Figure 1, is used to characterize the discharge behaviors of LiFePO_4 batteries [15]. The nonlinear open-circuit voltage source has a capacitor and a self-discharge resistor, as shown in the dashed line rectangle.

When a battery is connected to a load, as shown in Figure 1(b), there is an instantaneous drop in voltage caused by the current flowing through the equivalent series resistance, which is also the primary component of the battery's internal resistance. Therefore, the CCV is the difference between the open circuit voltage (OCV) and the voltage across the equivalent series resistor.

An RC network is composed of a resistor and a capacitor in parallel, and is used to investigate the transient responses when the battery is switched between the loading state (the closed circuit) and idle state (the open circuit). Multiple RC networks can be used, which closely captures the transient behavior but makes the calculation more complicated [15].

When the battery is connected to the load, the capacitor in the RC network begins charging and the voltage across the resistor in the RC network increases. Therefore, the CCV decreases. When the battery is disconnected from the load, there is no longer any current and the voltage is zero across the series resistor, R_{series} . The capacitor in the RC network is discharged by the parallel

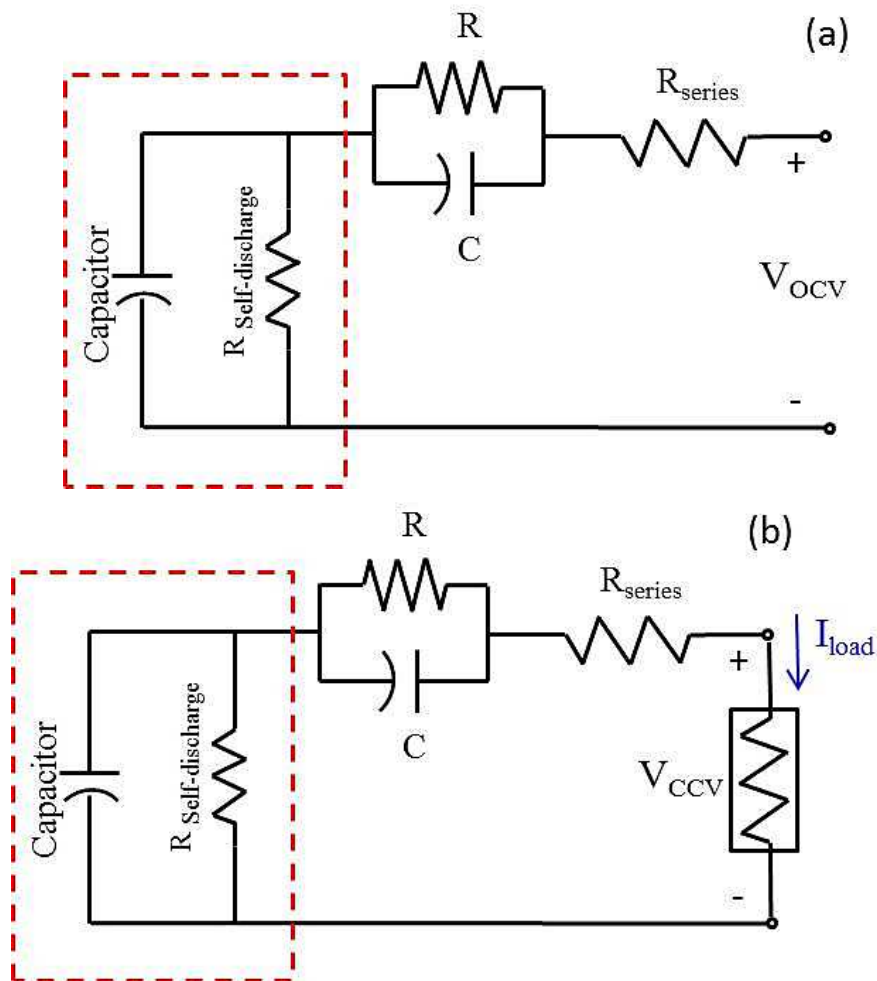


Figure 1: The electrical circuit model for a LiFePO₄ battery, which is a modification of the circuit of Schweighofer et al. [15], for an (a) open circuit and (b) closed circuit.

resistor and the voltage across the RC network decreases. Therefore, the measured voltage gradually recovers from a CCV state to an OCV state.

The equivalent series resistance, the combination of all resistance in the model shown in Figure 1, is

$$R_{\text{total}} = \frac{V_{\text{OCV}} - V_{\text{CCV}}}{I_{\text{load}}}. \quad (1)$$

From the electrical circuit model and experimental data, OCV, CCV and R_{total} are nonlinear functions of the discharge time, as shown in Figures 2. These curves are approximately the combination of an exponential term and a polynomial representing the equivalent capacitance and the equivalent resistance, respectively [15], so

$$\text{CCV}(t) = a \exp(bt + c) + dt^3 + et^2 + ft + g, \quad (2)$$

where a , b , c , d , e , f and g are parameters obtained by the fitting.

The LiFePO_4 batteries tested are classified into three types.

- New battery: a battery that has not been used and has not been stored for a year.
- Used battery: 300-cycle and 1000-cycle batteries that have been charged and discharged about 300 and 1000 times, respectively.
- Aged battery: one-year, three-year, and five-year batteries that have been stored without being charged or discharged for one, three and five years, respectively.

At the beginning of the experiment, each battery was charged using a DC power generator based on a constant-current (CC) constant-voltage (CV) method. The charging current and voltage were set to 10 A and 3.65 V, respectively. After the charging process, the battery was left idle for 24 hours to ensure that the initial voltage was in a steady state. The batteries were then discharged with a discharge current of 10 A through a DC electronic load. The data was recorded and collected via a computer using the LabVIEW software.

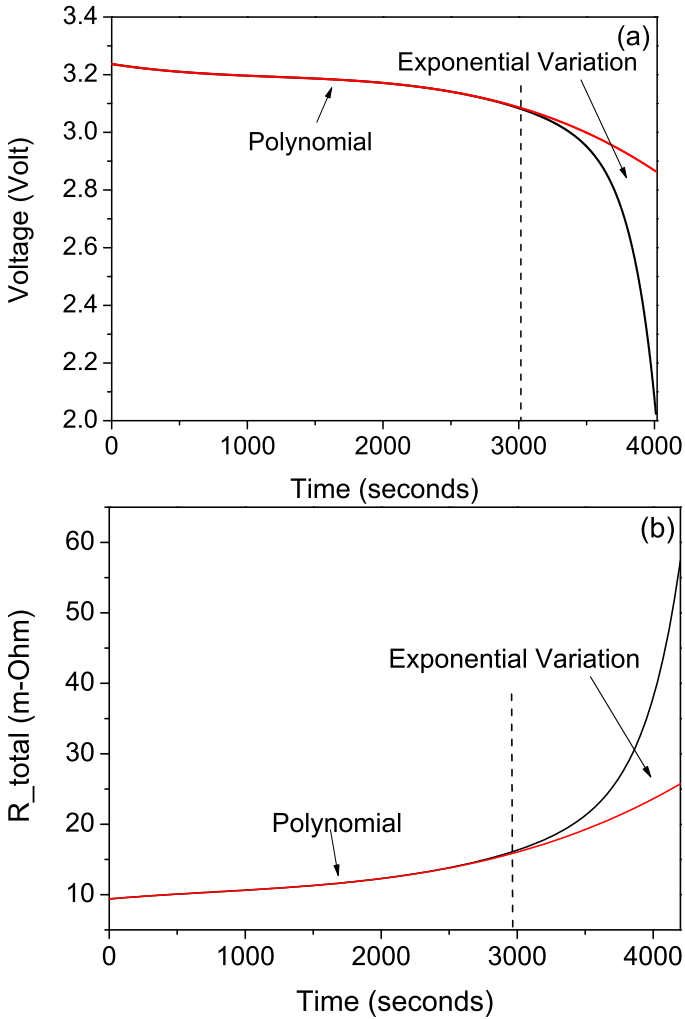


Figure 2: (a) The change of voltage and (b) the change in the equivalent series resistance during the discharge process.

3 Results and discussion

Using the discharge curve of a new battery generated during the experiment, the LabVIEW program fits the curve. The parameters of equation (2) obtained from the fitting process are $\mathbf{a} = -1.8 \times 10^{-5} \text{ V}$, $\mathbf{b} = 5.0256 \times 10^{-3} \text{ 1/s}$, $\mathbf{c} = -9.7$, $\mathbf{d} = -1.7 \times 10^{-11} \text{ V/s}^3$, $\mathbf{e} = 61.93 \times 10^{-9} \text{ V/s}^2$, $\mathbf{f} = -9.2 \times 10^{-5} \text{ V/s}$, and $\mathbf{g} = 3.161 \text{ V}$. The fitted curve closely matches the experimental data for a new battery, as shown in Figure 3. However, without any adjustments these parameters are not suitable for used and aged batteries. Figure 4 shows all the parameters from equation (2) obtained from the fitting processes for new, 300-cycle, 1000-cycle, one-year, three-year, and five-year batteries. The differences between most parameters are too small to distinguish the different batteries, and only \mathbf{c} , the order of the exponential term, requires significant adjustment. Therefore, to develop a mathematical model that is suitable for a range of batteries, rather than fitting all the discharge curves for the tested batteries, the above values are used for all tested batteries and then the exponential term and the polynomial terms in equation (2) are independently modified.

The dashed line in Figure 5(a) is the exponential function in equation (2). The exponential function dominates the discharge time (lifetime) of the batteries under various conditions. Therefore, the time shift property is used in shortening the lifetime of a battery, as shown by the solid line in Figure 5(a). Consequently, the modified exponential part of equation (2) is

$$\text{CCV}_{\text{exp}}(\mathbf{t}) = \mathbf{a} \exp[\mathbf{b}(\mathbf{t} - \Delta\mathbf{t}) + \mathbf{c}], \quad (3)$$

where $\Delta\mathbf{t}$ is a time shift.

The dashed line in Figure 5(b) is the polynomial function in equation (2). The polynomial function mainly dominates the change in the CCV. This means that the decay rate of the CCV at the sharp change region of the discharge curve is estimated by modifying the polynomial function. This estimation is very important because when the voltage starts to drop rapidly, the remaining

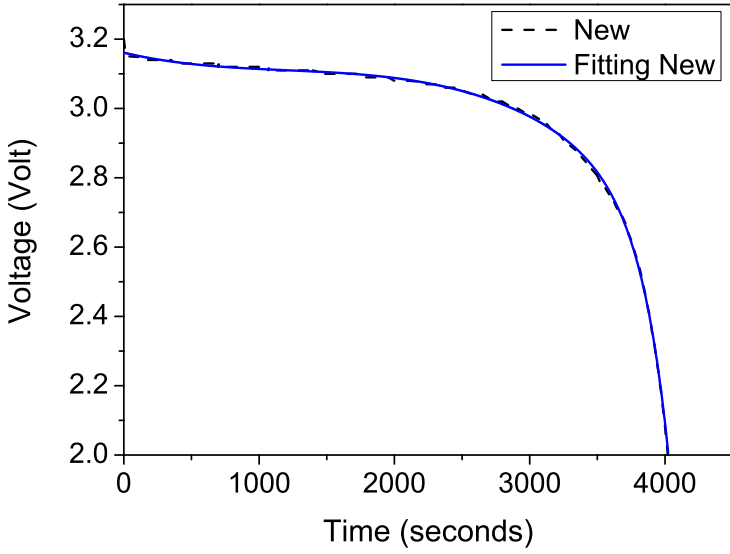


Figure 3: The fitting curve and experimental data curve for a new battery.

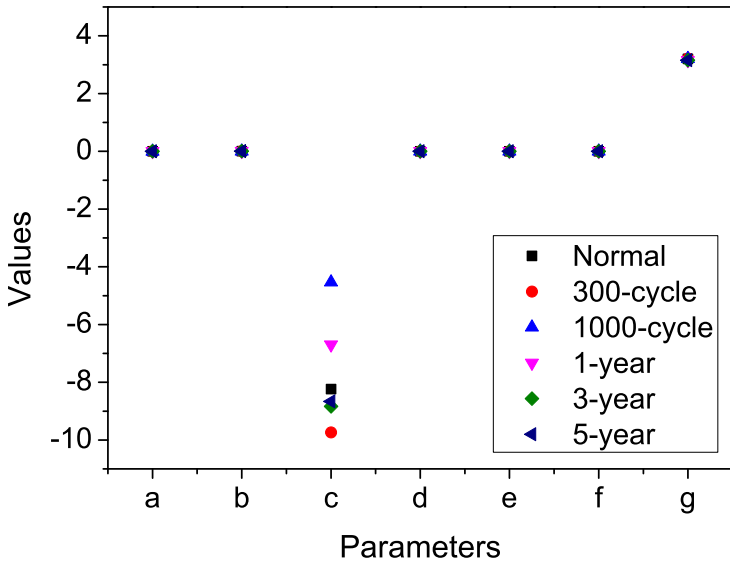


Figure 4: Different sets of parameters from equation (2) for all tested batteries.

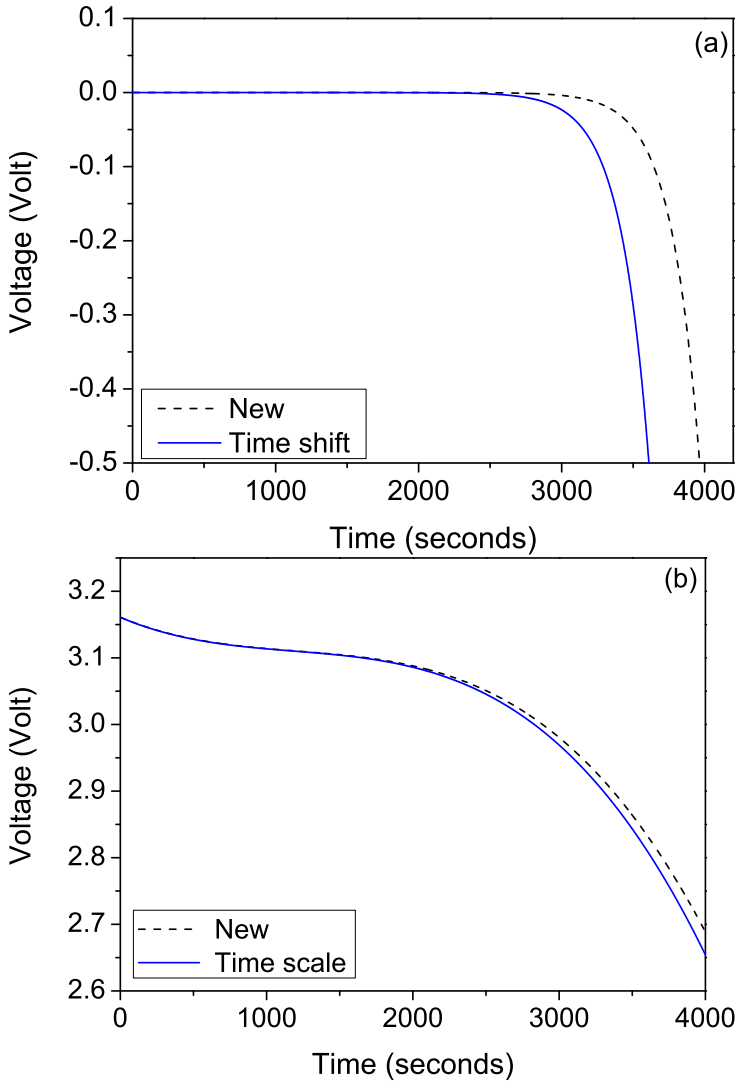


Figure 5: (a) The time shift applied to the exponential function to shorten the lifetime and (b) the time scale applied to the polynomial function to increase the decay rate of the CCV.

lifetime is very short, which has safety implication. The time scale process is used to enhance the change in CCV at the sharp change region of the discharge curve, as shown by the solid line in Figure 5(b). The modified equation for the polynomial part of equation (2) is

$$\text{CCV}_{\text{poly}}(t) = d(rt)^3 + e(rt)^2 + f(rt) + g, \quad (4)$$

where r is a time scale.

The modified equation for new, used and aged batteries is a combination of equations (3) and (4):

$$\text{CCV}_M(t) = a \exp[b(t - \Delta t)] + d(rt)^3 + e(rt)^2 + f(rt) + g. \quad (5)$$

Figure 6 shows that the fitted curve (pink solid line) for a one-year battery closely matches the experimental data curve (dashed line) after applying a time shift of $\Delta t = 355$ s and a time scale of $r = 1.02$. Figure 6 also shows the fitted curve (blue solid line) and the experimental data curve (dotted line) for a three-year battery. The two lines closely match after applying a time shift of $\Delta t = 1200$ s and a time scale of $r = 1.15$. However, the fitted curve (blue solid line) does not closely match the sharp change in gradient of the experimental data curve (dash-dotted line) for a five-year battery after applying a time shift of $\Delta t = 1250$ s and a time scale of $r = 1.2$. In addition, the lifetime does not match. Although the time shift could be increased to about 1290 s to exactly match the discharge time, this will enlarge the mismatch at the change of gradient. As mentioned above, the fitting at the gradient change is much more significant than the lifetime, and the mismatch for the lifetime is only 40 s, so the fitting is still acceptable.

Figure 7 shows fitted curves (colored solid lines) and experimental data curves (black dotted and dashed lines) for 300-cycle and 1000-cycle batteries. Both colored lines closely match the black lines after applying a time shift of $\Delta t = 450$ s and $\Delta t = 770$ s, and a time scale of $r = 1.05$ and $r = 1.16$ for 300-cycle and 1000-cycle batteries, respectively, indicating that this method is also suitable for analyzing the discharge behavior of used batteries.

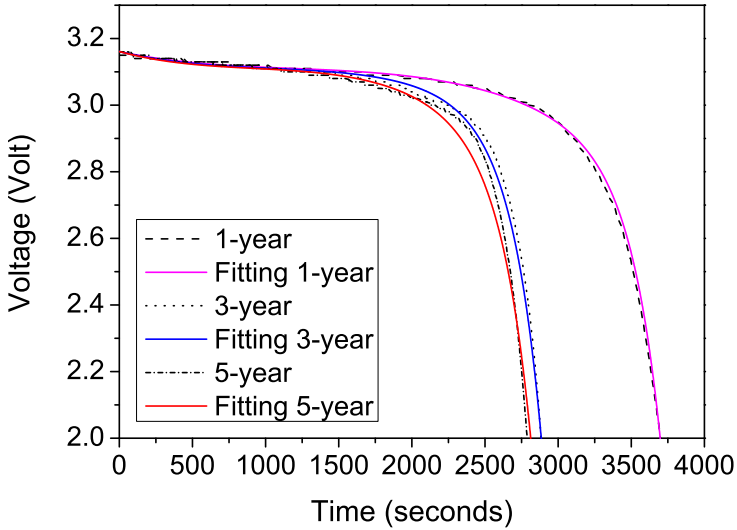


Figure 6: Three fitted curves and three experimental data curves for one-year, three-year, and five-year batteries.

Table 1: Time shift and time scale values for all tested batteries.

	new	1-year	3-year	5-year	300-cycle	1000-cycle
Time shift	0	355	1200	1250	450	770
Time scale	1	1.02	1.15	1.2	1.05	1.16

Table 1 lists the fitting results for the time shift and time scale values for all tested batteries. The lifetime of a battery reduces as the time shift value increases. Furthermore, when the battery is stored for more than three years, the lifetime barely changes, being only a little shorter than that of the three-year battery.

As the time scale increases, the voltage drop of the CCV also increases, and the worse the quality of the battery. This phenomenon is observed from the results for 1000-cycle and five-year batteries shown in Table 1. Therefore, it is very easy to characterize and distinguish batteries under various conditions

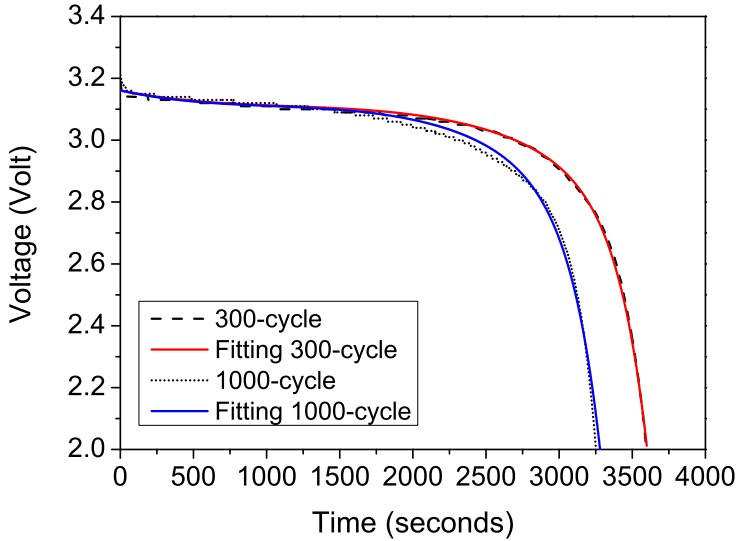


Figure 7: Fitted curves and experimental curves of 300-cycle and 1000-cycle batteries.

using the proposed method, compared with performing an analysis of all parameters of the batteries.

The percentage difference between the experimental and the fitted data during the discharge time is

$$\frac{1}{N} \sum \frac{|\text{CCV}_{\text{real}} - \text{CCV}_{\text{fit}}|}{\text{CCV}_{\text{real}}} \times 100\%, \quad (6)$$

where CCV_{real} is experimental data and CCV_{fit} is the fitting data and N is the total number of data records over the discharge time. The sum is over the whole discharge time.

The average and maximum percentage differences of CCV are listed in Table 2. As the parameters are determined relative to those of a new battery, the average and the maximum differences of the new battery are the lowest. The fitted data for other batteries, obtained using the same parameters, but with

Table 2: The percentage differences between the experimental and fitted data for all tested batteries

	new	1 year	3 year	5 year	300-cycle	1000-cycle
Average (%)	0.15	0.27	0.44	0.58	0.23	0.44
Maximum(%)	0.6	1.9	2.4	2.9	1.0	1.5

different time shifts and time scales, have larger differences than those of the new battery. The highest average difference is 0.58%. The maximum difference usually occurs near the gradient change of the discharge curve, as is the case for the five-year battery. The highest difference is about 2.9%, which means that the modified fitting method performs very well and is a very feasible approach.

4 Conclusions

A mathematical model was developed to investigate variations in the CCV during the discharge process for new, used and aged batteries by applying a time shift to the exponential term and a time scale to the polynomial terms. This model is used to satisfactorily capture the discharge behaviors of most tested batteries with an average error of less than 0.6%. In addition, this method can also be used to distinguish batteries under various conditions without the need to perform complicated calculations.

Acknowledgements This work was supported in part by the National Science Council of Taiwan under Grant NSC-102-2622-E-002-004-CC2.

References

- [1] W. Su, H. Eichi, W. Zeng and M.-Y. Chow, A survey on the electrification of transportation in a smart grid environment, *IEEE Intl. Conf. Ind. I.* 8:1–10, 2012. doi:[10.1109/TII.2011.2172454](https://doi.org/10.1109/TII.2011.2172454) C369
- [2] J. Wang, Z. Sun and X. Wei, Performance and characteristic research in LiFePO₄ battery for electric vehicle applications, *IEEE Vehicle Power* 1657–1661, 2009. doi:[10.1109/VPPC.2009.5289664](https://doi.org/10.1109/VPPC.2009.5289664) C369
- [3] A. Shafiei, A. Momeni and S. S. Williamson, Battery modeling approaches and management techniques for plug-in hybrid electric vehicles, *IEEE Vehicle Power* 1–5, 2011. doi:[10.1109/VPPC.2011.6043191](https://doi.org/10.1109/VPPC.2011.6043191) C369
- [4] P. Bai, D. A. Cogswell and M. Z. Bazant, Suppression of phase separation in LiFePO₄ nanoparticles during battery discharge, *Nano Lett.* 11:4890–4896, 2011. doi:[10.1021/nl202764f](https://doi.org/10.1021/nl202764f) C369
- [5] H. L. Chan and D. Sutanto, A new battery model for use with battery energy storage systems and electric vehicle power systems, *IEEE Power Eng. Soc.* 1:470–475, 2000. doi:[10.1109/PESW.2000.850009](https://doi.org/10.1109/PESW.2000.850009) C369
- [6] T. Kim and W. Qiao, A hybrid battery model capable of capturing dynamic circuit characteristics and nonlinear capacity effects, *IEEE T. Energy Conver.* 26:1172–1180, 2011. doi:[10.1109/TEC.2011.2167014](https://doi.org/10.1109/TEC.2011.2167014) C369
- [7] D. N. Rakhmatov and S. B. K. Vrudhula, An analytical high-level battery model for use in energy management of portable electronic systems, *IEEE ICCAD* 488–493, 2001. doi:[10.1109/ICCAD.2001.968687](https://doi.org/10.1109/ICCAD.2001.968687) C369
- [8] V. Srinivasan and J. Newman, Discharge model for the lithium iron-phosphate electrode, *J. Electrochem. Soc.* 151:A1517–A1529, 2004. doi:[10.1149/1.1785012](https://doi.org/10.1149/1.1785012) C369

- [9] V. Rao, G. Singhal, A. Kumar and N. Navet, Battery model for embedded systems, *VLSI Des.* 105–110, 2005. doi:[10.1109/ICVD.2005.61369](https://doi.org/10.1109/ICVD.2005.61369)
- [10] S. Dargavillez and T. W. Farrell, Predicting active material utilization in LiFePO₄ electrodes using a multiscale mathematical model, *J. Electrochem. Soc.* 157:A830–A840, 2010. doi:[10.1149/1.3425620](https://doi.org/10.1149/1.3425620)
- [11] R. Rao, S. Vrudhula and D. N. Rakhmatov, Battery modeling for energy-aware system design, *Computer* 36:77–87, 2003. doi:[10.1109/MC.2003.1250886](https://doi.org/10.1109/MC.2003.1250886)
- [12] M. Chen and G. A. Rincon-Mora, Accurate electrical battery model capable of predicting runtime and i-v performance, *IEEE T. Energy Conver.* 21:504–511, 2006. doi:[10.1109/TEC.2006.874229](https://doi.org/10.1109/TEC.2006.874229)
- [13] L. Gao, S. Liu and R. A. Dougal, Dynamic lithium-ion battery model for system simulation, *IEEE T. Compon. Pack. T.* 25:495–505, 2002. doi:[10.1109/TCAPT.2002.803653](https://doi.org/10.1109/TCAPT.2002.803653)
- [14] V. Agarwal, K. Uthaichana, R. A. DeCarlo and L. H. Tsoukalas, Development and validation of a battery model useful for discharging and charging power control and lifetime estimation, *IEEE T. Energy Conver.* 25:821–835, 2010. doi:[10.1109/TEC.2010.2043106](https://doi.org/10.1109/TEC.2010.2043106)
- [15] B. Schweighofer, K. M. Raab and G. Brasseur, Modeling of high power automotive batteries by the use of an automated test system, *IEEE T. Instrum. Meas.* 52:1087–1091, 2003. doi:[10.1109/TIM.2003.814827](https://doi.org/10.1109/TIM.2003.814827)

Author addresses

1. **Shin-Yi Lee**, Department of Education, University of Taipei, Taipei 10048, Taiwan.
<mailto:sylee@utapei.edu.tw>

2. **Wei-Li Chiu**, Department of Engineering Science and Ocean Engineering, National Taiwan University, Taipei 10617, Taiwan.
<mailto:r01525038@ntu.edu.tw>
3. **Yi-Shuo Liao**, Department of Engineering Science and Ocean Engineering, National Taiwan University, Taipei 10617, Taiwan.
<mailto:dhjlin@ntu.edu.tw>
4. **Kung-Yen Lee**, Department of Engineering Science and Ocean Engineering, National Taiwan University, Taipei 10617, Taiwan.
<mailto:kylee@ntu.edu.tw>
5. **Jau-Horng Chen**, Department of Engineering Science and Ocean Engineering, National Taiwan University, Taipei 10617, Taiwan.
<mailto:jauchen@ntu.edu.tw>
6. **Huei-Jeng Lin**, Department of Engineering Science and Ocean Engineering, National Taiwan University, Taipei 10617, Taiwan.
<mailto:hjlin@ntu.edu.tw>
7. **Kang Li**, Department of Mechanical Engineering, National Taiwan University, Taipei 10617, Taiwan.
<mailto:kangli@ntu.edu.tw>